

## Article

# Effect of Processing Routes on Physical and Mechanical Properties of Advanced Cermet System

Vikas Verma <sup>1</sup>, Margarita García-Hernández <sup>2</sup>, Jorge Humberto Luna-Domínguez <sup>3,\*</sup>,  
Edgardo Jonathan Suárez-Domínguez <sup>4</sup>, Samuel Monteiro Júnior <sup>5</sup> and Ronaldo Câmara Cozza <sup>6</sup>

<sup>1</sup> Aqila Technologies and Integration Solutions Private Limited, Department of Aerospace Design & Operations, Noida 201301, Uttar Pradesh, India; vikasverma.iitr@rediffmail.com

<sup>2</sup> Instituto Politécnico Nacional, CECyT 16 “Hidalgo” Distrito de Educación, Salud, Ciencia, Tecnología e Innovación, Carretera Pachuca Actopan Km 1 + 500, San Agustín Tlaxiaca C.P. 42162, Hidalgo, Mexico; margaciah@ipn.mx

<sup>3</sup> Facultad de Odontología, Universidad Autónoma de Tamaulipas, Av. Universidad esq. con Blvd. Adolfo López Mateos s/n, Tampico C.P. 89337, Tamaulipas, Mexico

<sup>4</sup> Facultad de Arquitectura, Diseño y Urbanismo, Universidad Autónoma de Tamaulipas, Av. Universidad esq. con Blvd. Adolfo López Mateos s/n, Tampico C.P. 89337, Tamaulipas, Mexico; edgardo.suarez@docentes.uat.edu.mx

<sup>5</sup> Centro Universitário das Faculdades Metropolitanas Unidas—FMU, Departamento de Engenharia Mecânica, Rua Afonso Braz 889, São Paulo 04511-011, SP, Brazil; samuel\_monteiro@terra.com.br

<sup>6</sup> CEETEPS—State Center of Technological Education “Paula Souza”, Department of Mechanical Manufacturing, Av. Antônia Rosa Fioravante 804, Mauá 09390-120, SP, Brazil; ronaldo.cozza@fatec.sp.gov.br

\* Correspondence: jhluna@docentes.uat.edu.mx

**Abstract:** The present research focuses on the effects of different processing routes on the physical and mechanical properties of nano Ti(CN)-based cermets with metallic binders. Tungsten carbide (WC) is added as a secondary carbide and Ni-Co is added as a metallic binder to nano Ti(CN)-based cermet processed via conventional and spark plasma sintering (SPS). A systematic comparison of the composition and sintering conditions for different cermets’ systems was carried out to design novel composition and sintering conditions. Nano TiCN powder was prepared by 30 h of ball milling. The highest density of >98.5% was achieved for the SPS-processed cermets sintered at 1200 °C and 1250 °C for 3 min at 60 MPa of pressure in comparison to the conventionally sintered cermets at 1400 °C for 1 h with a two-stage compaction process—uniaxially at 150 MPa and isostatically at 300 MPa of pressure. Comparative X-ray diffraction (XRD) analysis of the milled powders at different time intervals was performed to understand the characteristics of the as-received and milled powders. Peak broadening was observed after 5 h of ball milling, and it increased to 30 hr. Also, peak broadening and a refined carbide size was observed in the XRD and scanning electron microscope (SEM) micrographs of the SPS-processed cermet. Transmission electron microscope (TEM) analysis of the milled powder showed that its internal structure had a regular periodic arrangement of planes. SEM base scattered electron (BSE) images of all the cermets primarily showed three major microstructural phases of the core–rim–binder with black, grey, and white contrast, respectively. With the present sintering conditions, a high hardness of ~16 GPa and a fracture toughness of ~9 MPa m<sup>1/2</sup> were obtained for SPS-processed cermets sintered at higher temperatures.

**Keywords:** cermet system; spark plasma sintering; metal–ceramic bond; ball milling; ceramics



**Citation:** Verma, V.; García-Hernández, M.; Luna-Domínguez, J.H.; Suárez-Domínguez, E.J.; Monteiro Júnior, S.; Câmara Cozza, R. Effect of Processing Routes on Physical and Mechanical Properties of Advanced Cermet System. *Ceramics* **2024**, *7*, 625–638. <https://doi.org/10.3390/ceramics7020041>

Academic Editor: Gilbert Fantozzi

Received: 31 January 2024

Revised: 29 March 2024

Accepted: 3 April 2024

Published: 2 May 2024



**Copyright:** © 2024 by the authors. Licensee MDPI, Basel, Switzerland. This article is an open access article distributed under the terms and conditions of the Creative Commons Attribution (CC BY) license (<https://creativecommons.org/licenses/by/4.0/>).

## 1. Introduction

Titanium carbonitride-based cermets are considered candidate materials for machining purposes in the tool industry because they possess high mechanical properties and high wear performance [1,2].

An attempt has been made to process densified “micro” and “nano” Ti(CN)-based cermet with the addition of secondary carbides and metallic binders [3,4]. Generally, with

ceramics, nickel (Ni) and cobalt (Co) are used as binders as they have high wettability with ceramic phase, although the fundamental binder with maximum wettability in the ceramic phase is Ni. During sintering at high temperatures, liquid Ni-Co spreads over the surface of hard phase, resulting in a strong metal ceramic bond. In Ti(CN) cermet, tungsten carbide (WC) is added as a secondary carbide; it is readily wetted by both molten nickel and cobalt during sintering and improves the sinterability [4–6]. Ahn and Kang et al. [7,8], in their research, reported that during sintering, core–rim–binder morphology arises. Conventional processing, a cost-effective technique, is always preferred for processing as it is suitable for bulk production, and components of different sizes and shapes can easily be fabricated [9]. A higher compaction load leads to an increase in densification by eliminating large pores [10]. A design of an apparatus used for processing was provided by Yoo et al. [11,12]. It includes a chamber, a punch and die assembly for supporting a particle material, plungers for applying shear and/or axial pressures, and a power supply for applying a current. Currently, the spark plasma sintering (SPS) technique is becoming popular as it fabricates a densified product in a short processing time and at a lower sintering temperature [13–15]. Alvarez et al. [13] processed densified Ti(C, N) cermets with metallic binders with a submicron particle size via SPS at 100 MPa of uniaxial pressure for 2 min at a 1400 °C sintering temperature. Ping et al. [14] processed nano Ti(CN)-Mo/Ni cermet via SPS at 1050 °C to 1450 °C for 3 min at 30 MPa of pressure. Porosity was found to be negligible at 1200 °C. A perfect external appearance of the sintered samples under 1350 °C was observed, but cracks were visible above 1430 °C. Zheng et al. [15] processed nano Ti(CN) cermet with WC, Ni, Mo, VC, and graphite addition via SPS. It was observed that the particle size of the constituents and plasma pressure to be applied for the compaction also effects the properties of processed materials. In a case of processing bulk tungsten samples, it was observed that under identical processing conditions (pressure applied, temperature, and processing time) the presence of porosity was randomly distributed throughout the microstructure, and a density of 92 pct to 96 pct was achieved. For a tungsten sample that was obtained by consolidating powders with an initial size of 275 nm, porosity was evident throughout the agglomeration of both the macroscopic and fine microscopic pores [16,17]. A literature survey shows that the field of processing nano Ti(CN)-based cermets is still to be explore-considering, for example, conditions where is necessary the knowledge of the fracture toughness behavior [18]. Table 1 Shows the summary of composition and sintering conditions of investigated cermets' systems. Table 2 Shows the summary of properties of investigated cermets' systems.

**Table 1.** Summary of composition and sintering conditions of investigated cermets' systems.

Powder Info			Composition Info	Milling Parameters			Sintering			Paper Info (Year)	Ref.
TiCxNi1-x, $\mu\text{m}$	X	WC, $\mu\text{m}$		Velo (RPM)	Time (h)	Tech Used	Pressure (MPa)	Sintering Temp	Holding Time (min)		
>0.1	0.7	0.85	TiCN-43,WC-6.9,Ni-32,Mo-16,VC-0.6,C-1.5	200	24 h	SPS	20	1350	3	2004	[15]
3–4	0.5	1–4	TiCN-65,WC-15,Ni-20	250	20	VS	150	1510	60	2004	[19]
1	0.7	0.8	TiCN-WC-Mo2C-(Co,Ni)	-	80	VS	100	1360	60	2008	[20]
0.1	0.5	1.14	TiCN-(47.5–57.5),WC-20,Co-15,Mo-(5–15),C-2.5	-	24 h	VS	170	1430	60	2006	[21]
<1	0.7	<1	TiCN-59,WC-15,Co + Ni-17,Mo2C-9	304	50 h	VMS	300	1400	5	2009	[22]
0.8–3	0.5	5.9	TiCN-50,WC-21.22,Ni-20,{Mo + Ta(Nb)}-8.47	-	24 h	VS	125	1510	60	2012	[23]
0.7–0.95	0.5	0.4	TiCN-55,WC-25,Ni-20	-	24 h	VS	100	1510	60	2001	[24]

Table 1. Cont.

Powder Info			Composition Info	Milling Parameters			Sintering			Paper Info (Year)	Ref.
TiCxNi1-x, $\mu\text{m}$	X	WC, $\mu\text{m}$		Velo (RPM)	Time (h)	Tech Used	Pressure (MPa)	Sintering Temp	Holding Time (min)		
0.13	0.7	0.45	TiCN-53.5,WC-15,Co + Ni-14.5,TaC-7,Mo2C-10	-	45 h	VS	-	1450	60	2008	[25]
0.5–0.8	0.5	200 nm	TiCN-51.87,WC-16,Ni-11,Co-9,Mo2C-12,VC-0.13	30	72 h	VS	120	1450	90	2010	[26]
0.3	0.7	0.2	TiCN-55,WC-25,Ni-20	-	24 h	VS	100	1510	60	2003	[27]
0.13	0.7	0.45	TiCN-X, Ni + Co-14.5,Mo2C-10, (WC-15/TaC-10)	68	48 h	VS	-	-	-	2006	[28]
1	0.7	0.2	TiCN-51.4,WC-15,Co + Ni-15,Mo2C-10,TaC-8,Ce/Co-0.6	-	72 h	VS	100	1465	60	2012	[29]
-	0.5	-	TiCN-85,Co-15	400	30 min	SPS	80	1300	1	2012	[30]
-	0.5	-	TiCN-80.75,Al2O3-14.25,Mo-2.5,Ni-2.5	-	-	SPS	50	1450	2	2003	[31]
0.7	0.8	3.52	TiCN-65,WC-15,Ni-7.5,Co-7.5,Mo-4,C-1	150	24 h	VS	180	1430	60	2006	[32]
1	0.7	0.72	TiCN-43,WC-6.9,Ni-32,Mo-16,Cr3C2-0.6,C-1.5	150	12 h	VS	300	1450	60	2004	[33]
TiC-3.87, TiN-0.04	0.5	3.25	TiCN-X,WC-15,Co + Ni-24, Mo-8/15,	-	24 h	VS	170	1450	60	2004	[34]
0.5	0.7	0.45	TiCN-53.5,WC + TaC-22,Ni + Co-14.5,Mo2C-10	68	48 h	VS	-	-	-	2005	[35]
TiC-1.5, TiN-2.9	0.5	-	TiCN-70,Ni-20,Mo2C-10	-	24 h	VS	100	1550	120	2008	[36]
0.21	0.7	-	TiCN-76,Ni-12,Mo2C-12	-	36 h	SPS	30	1250	3	2003	[37]

VS-Vacuum Sintering.

Table 2. Summary of physical and mechanical properties of investigated cermets' systems.

Composition	Properties of Sintered Cermets						Ref.
	% Density	Relative Density ( $\text{gm/cm}^3$ )	Grain Size ( $\mu\text{m}$ )	Hardness (GPa)	Fracture Toughness ( $\text{MPa}\cdot\text{m}^{1/2}$ )	Trans R.S. MPa	
TiCN-76,Ni-12,Mo2C-12	-	-	0.42	16.78	-	295	[14]
TiCN-43,WC-6.9,Ni-32,Mo-16,VC-0.6,C-1.5	-	6.48	>100 nm	14.2	-	879.5	[15]
TiCN-65,WC-15,Ni-20	98.8	6.16	30–100 nm	12.2	12	-	[19]
TiCN–WC–Mo2C–(Co,Ni)	-	-	-	-	-	-	[20]
TiCN-57.5,WC-20,Co-15,Mo-5, C-2.5	-	-	1.17	15.98	13.2	870	[21]
TiCN-52.5,WC-20,Co-15,Mo-10,C-2.5	-	-	1.15	17.39	11.9	990	[21]
TiCN-47.5,WC-20,Co-15,Mo-15,C-2.5	-	-	0.79	17.87	11	1030	[21]
TiCN-59,WC-15,Co + Ni-17,Mo2C-9	99.5	-	>1	17.36	-	-	[22]
TiCN-50,WC-21.22,Ni-20,{Mo + Ta(Nb)}-8.47	-	-	1–4	~11	~10	-	[23]
TiCN-55,WC-25,Ni-20	-	6.5	0.7–0.9	14.2	8.8	-	[24]
TiCN-53.5,WC-15,Co + Ni-14.5,TaC-7,Mo2C-10	-	6.39	>1	17.54	-	965	[25]

Table 2. Cont.

Composition	Properties of Sintered Cermets						Ref.
	% Density	Relative Density (gm/cm <sup>3</sup> )	Grain Size (μm)	Hardness (GPa)	Fracture Toughness (MPa·m <sup>1/2</sup> )	Trans R.S. MPa	
TiCN-51.87,WC-16,Ni-11,Co-9,Mo2C-12,VC-0.13	99.5	6.74	0.5–1	14.7	10.1	2210	[26]
TiCN-55,WC-25,Ni-20	-	-	1.2	14	7.3	-	[27]
TiCN-60.5,WC-15,Ni + Co-14.5,Mo2C-10	-	-	0.5	18.63	-	1500	[28]
TiCN-75.5,Ni + Co-14.5,Mo2C-10	-	-	0.5	18.7	-	1320	[28]
TiCN-50.5,WC-15,Ni + Co-14.5,Mo2C-10, TaC-10	-	-	0.5	18.65	-	1600	[28]
TiCN-51.4,WC-15,Co + Ni-15,Mo2C-10, TaC-8, Ce/Co-0.6	-	-	1–2	17.06	9.21	1639	[29]
TiCN-85,Co-15	99	-	>1	17.1	5.51	904	[30]
TiCN-80.75,Al2O3-14.25,Mo-2.5,Ni-2.5	-	5.115	0.5>	14.45	-	-	[31]
TiCN-65,WC-15,Ni-7.5,Co-7.5,Mo-4,C-1	-	6.258	>1	18.63	14.5	1623.5	[32]
TiCN-43,WC-6.9,Ni-32,Mo-16,Cr3C2-0.6,C-1.5	98>	-	>1	12.3	-	2884	[33]
TiCN-53,WC-15,Mo-8,Co + Ni-24	-	-	1	12.5	17	1425	[34]
TiCN-46,WC-15,Mo-15,Co + Ni-24	-	-	1	12.74	18.2	1600	[34]
TiCN-53.5,WC + TaC-22,Ni + Co-14.5,Mo2C-10	-	6.7	0.3	19.5	10.6	1740	[35]
TiCN-70,Ni-20,Mo2C-10	>98	5.56	3.2	-	14.2	-	[36]

There are also some challenges in the development of nano materials. The selection of an economical route of synthesis to obtain non-agglomerated nanocrystalline ceramic powders is the primary concern. To obtain the dense compaction of nanoparticles while avoiding cracks and inhibiting grain growth to achieve full densification is also a major issue. In regard to nano composites, their mechanical properties have yet to show improvements that meet expectations, which is why they have not yet penetrated the commercial market in a big way. SPS is a fast densification route that prevents the excessive grain growth encountered by nanocrystalline powders during sintering. The suppression of particle/grain coarsening while augmenting densification is essential. Lowering the sintering time and temperature is the solution, for which SPS proves to be suitable. By utilizing nano-scale WC and graphene nanosheets (GNSs) as additives, cermets were created via SPS [38]. Their hardness and fracture toughness were found to be greatly increased, by 44.58% and 92.73%, respectively, when compared to the specimen without GNSs. By promoting the migration of hard phases in the liquid phase and preventing their solubility and grain development, a specific concentration of GNSs can significantly boost the fracture toughness of ceramic materials. The characteristics of cermets appeared to be improved, and the creation of a (Ti, W) (C, N) rim phase is encouraged by the addition of nano-WC. Ti(C, N) and WC were progressively dissolved into liquid-phase Co during the liquid phase sintering stage, and they precipitated as a (Ti, W) (C, N) solid solution to produce a rim phase. It was concluded by the authors that cermets' mechanical characteristics can be enhanced, and the diffusion and densification of elements encouraged by the creation of this rim phase and sample densification can also be accelerated, with enhancement in the mechanical characteristics using SPS and adding nano-WC. The development of different core–rim morphologies in processed cermets was observed by reinforcing the produced ceramics with cubic  $\beta$ -cobalt ( $\beta$ -Co) as the binder phase [39]. Powders of (Ti, W, Mo, Ta) and (C, N) were added simultaneously to generate two different core–rim morphologies in an effort to improve the microstructure. Here, high-energy ball milling produced  $\beta$ -cobalt powders with face-centered cubic structures through a solid-phase reaction. The (Ti, W, Mo, Ta) (C, N) powders were made using a carbothermic reduction–nitridation process

and a solid-phase chemical reaction. To create Ti(C, N)-based ceramics with two types of core–rim structures—a black core/white rim and a white core/gray rim, the cobalt and (Ti, W, Mo, Ta) (C,N) powders were mixed, pressed and conventionally sintered, resulting in improved toughness and performance. TiN and nano-TiB<sub>2</sub> additions to titanium carbonitride (TiCN-WC-Cr<sub>3</sub>C<sub>2</sub>-Co)-based ceramics subjected to (SPS processing have been found to have specific effects [40]. TiN and nano-TiB<sub>2</sub> additions together affected the mechanical properties, with a 0 to 15 weight percent. When TiN was added, the fracture toughness value increased more than when nano-TiB<sub>2</sub> was added. On the other hand, cermets generated with the inclusion of nano-TiB<sub>2</sub> had higher hardness values. These outcomes indicate that the new ceramics function and are extremely tough. Also, sintered primarily Ti(C,N)-based cermets have been suggested to have advanced oxidation resistance, which may be further improved via the addition of alloyed Cr [41]. Four united cermets comprising Ti(C,N) at the earthenware stage and four high entropy combinations at the folio stage were synthesized by Obra et al. [42]. Mechanical alloying was used to create the four high entropy alloys (HEAs)—CoCrCuFeNi, CoCrFeNiV, CoCrFeMnNi, and CoFeMnNiV—which resulted in the formation of a single (face-centered cubic) fcc phase. Cold welding caused the materials to become highly agglomerated; however, the particles were made up of misoriented nanocrystalline domains that were roughly 10–50 nm in size. Porosity persisted in the majority of the cermets even though a high temperature of 1575 °C was needed to achieve the maximum cermet densification through pressureless sintering. Distinct compositional shifts were noted in the ceramic and binder phases during liquid-phase sintering with a core–rim microstructure in processed cermets. It was determined that cermet is a sophisticated class of material that combines the benefits of both metal and ceramic phases [43]. Cermets are composed of a hard ceramic phase and a metallic binding phase. This class of materials' outstanding qualities are especially helpful in tribological, machining, and high-temperature applications. Powder metallurgy (PM), reaction synthesis (RS), thermal spray (TS), cold spray (CS), and laser-based additive manufacturing techniques are the most widely used processing methods for cermet systems. Cermets are a type of material that minimizes the drawbacks of both ceramics and the metals while combining the benefits of both ceramic phase and metallic binder. Modern technologies have partially addressed the inherent challenges of producing components with both metal and ceramic phases.

A survey of the literature revealed that a great deal of research has been carried out to comprehend the mechanical behavior and processing of TiCN-based cermets via the conventional technique, but very little literature was found regarding the processing of nano TiCN-based cermets by SPS. TiCN-based cermets have been given consideration in recent years for their use in cutting tool applications because of their exceptional toughness, chemical stability at high temperatures, high hardness, increased wear resistance, and thermal shock resistance. In addition to their primary use in cutting tool industries for high-speed tool inserts and die making, TiCN-based ceramics are currently employed in the production of gauges, hot rolls, bearings, wire drawings, and refractory parts for diesel, gasoline, turbine, and jet engines. They are preferred in the mining and oil industries for use in drills, digging equipment, and oil pipeline nozzles and throttles. TiCN-based cermet cutting tools are different from conventionally used WC tools. They are reported to be more effective in specific cutting operations, such as surface finishing, having high wear resistance and a chemical inert nature against corrosion in comparison to WC tools. In the present work, an attempt has been made by the authors to obtain a deeper understanding and scientific findings on processing nano TiCN-based cermets with improved physical and mechanical properties via advanced the spark plasma technique in comparison to the same processed via conventional techniques. After a vast literature review, a preliminary composition was designed with addition of WC as secondary carbide and Ni-Co as metallic binders to nano Ti(CN). A thorough investigation was carried out to comprehend the compositional variations and processing techniques involved in producing

TiCN-based cermets via the PM approach. Table 3 present summaries Summary of patents of investigated cermets' systems.

**Table 3.** Summary of patents of investigated cermets' systems.

S. No.	Patent Ref.	Filing Date	Publication Date	Applicant	Title	Ref. No.
1	US2033513	12 June 1935	10 March 1936	Firth Sterling Steel Co.	Hard cemented carbide material	[44]
2	US4145213	17 May 1976	20 March 1979	Sandvik Aktiebolag	Wear-resistant alloy	[45]
3	US4942097	14 October 1987	17 July 1990	Kennametal Inc.	Cermet cutting tool (TiCN,WC,TiC,Mo2C,Co,Ni)	[46]
4	US4948425	6 April 1989	14 August 1990	Agency of Industrial Science and Technology	Titanium carbo-nitride and chromium carbide-based ceramics containing metals (TiC.5N.5,Cr3C2,Mo2C,B4C,Co,Ni,Si)	[47]
5	US5186739	21 February 1990	16 February 1993	Sumitomo Electric Industries, Ltd.	Cermet alloy containing nitrogen	[48]
6	US5370719	16 November 1993	6 December 1994	Mitsubishi Materials Corporation	Wear-resistant titanium carbonitride-based cermet cutting insert (TiCN,WC,Cr3C2,Mo2C,ZrC,TaC,NbCN,VC,Ni,Co)	[49]
7	US5395421	30 September 1993	7 March 1995	Sandvik Ab	Titanium-based carbonitride alloy with controlled structure (TiC,TiN,WC,Mo2C,TaC,VC,Co,Ni)	[50]
8	US5766742	31 October 1996	16 June 1998	Mitsubishi Materials Corporation	Cutting blade made of titanium carbonitride-base cermet, and cutting blade made of coated cermet (TiCN,TiN,TaC,NbC,WC,VC,ZrC,Cr3C2,Mo2C,Co,Ni, graphite powder C)	[51]
9	US6004371	19 January 1996	21 December 1999	Sandvik Ab	Titanium-based carbonitride alloy with controllable wear resistance and toughness (TiC,TiN,WC,Mo2C,TaC,VC,Co,Ni)	[52]
10	US 6,387,552 B1	21 September 2000	14 May 2002	Hitachi Tool Engineering, Ltd., Tokyo (JP)	TiCN-Based Cermet (TiN,TiC,TiCN,WC,MoC,TaC,Ni,Co)	[53]
11	EP1043414A1	5 April 2000	11 October 2000	Mitsubishi Materials Corporation	Cermet cutting insert	[54]
12	US7332122	7 October 2003	19 February 2008	Sandvik Intellectual Property Ab	Ti(C,N)-(Ti,Nb,W)(C,N)-Co alloy for milling cutting tool applications	[55]
13	EP3 181 274B1	2 April 2015	18 December 2019	Nano Tech Co., Ltd.	Method For Producing Titanium Carbonitride Powder (TiO <sub>2</sub> ,Ca,C,N <sub>2</sub> )	[56]
14	US7645316	30 October 2006	12 January 2010	Sandvik Intellectual Property Aktiebolag	Ti(C,N)-(Ti,Nb,W)(C,N)-Co alloy for finishing and semifinishing turning cutting tool applications	[57]
15	US8007561	13 June 2006	30 August 2011	Ngk Spark Plug Co., Ltd.	Cermet insert and cutting tool	[58]
16	US 8202344 B2	21 May 2007	19 June 2012	Kennametal Inc.	Cemented carbide with ultra-low thermal conductivity (TiC,WC,Cr3C2,TaNbC,Mo2C,Ni,Co)	[59]

## 2. Materials and Methods

Commercially available Ti(CN), WC, Ni, and Co powders of sub-micron particle size from Stark and Aldrich were used and the following cermet composition (wt%) was designed for investigation: 75TiCN-10WC-15(Ni-Co). Ti(CN) powder with a 1–2 μm size was systematically milled in high-energy ball mill machine (PM100, Retsch, Haan, Germany) consecutively for 1, 5, 10, 15, 20, 25, and 30 h to obtain non-agglomerated, ultra-fine (nano) powder with narrow size distribution and minimum contamination.

The conventional method of processing was chosen in this research work as it is a low-cost manufacturing technique that can create a large variety of sintered shapes for large quantities with ease of fabrication, providing excellent geometric accuracy, surface finish, and the efficient use of materials, but it results in considerable grain coarsening during the processing, which effects the physical and mechanical properties. In this regard, the SPS technique has emerged as a novel processing route, employing a rapid rate of heating and lowering the holding time at the sintering temperature, completing densification within a few minutes. A relatively low sintering temperature with a rapid processing time permits tight control of the grain growth and microstructure. For the conventional sintering process, the mixed powders were uniaxially compacted at 150 MPa and further cold-pressed isostatically at 300 MPa in the PTR D100/440/12 Tube Furnace (Program Thermal Tech Co., Ltd., Luoyang, China) to achieve uniform density in the compacts. Samples with a 4–6 mm thickness were prepared and subsequently sintered at a 1400 °C temperature for a 60 min holding time in an inert atmosphere. The spark plasma sintering experiments were performed at 1200 °C and 1250 °C for 3 min at 60 MPa of pressure using SPS (Phenom Pharos, Nanoscience Instruments, Phoenix, AZ, USA). The SPS process was a multistage regime (non-linear), with holding periods at 800 °C (4 min) with a constant 60 MPa of pressure. Multistage SPS promotes the activation of grain boundaries, and their diffusion leads to a densified bonded structure. The cermet samples were thoroughly polished. The Vickers hardness was measured at a 10 kg load using a hardness tester (QNESS 200 CS, QTAM, Mammelzen, Germany). Indent images were seen on an optical microscope, and the hardness was calculated by the formula given in Equation (1). Shetty et al. [18]’s formula given in Equation (2) was applied to calculate the fracture toughness value. The average values of five readings are reported. Using a Vickers diamond pyramid indenter, the indentation fractures of a number of well-characterized cermets were investigated. The obtained crack length–indentation load data were examined using relationships typical of fully developed radial/median crack geometries and radial crack geometries. For every alloy under investigation, the radial crack model provided a better fit to the data. It was demonstrated that the observed linear relationship between the radial crack length and the indentation load is consistent with an indentation fracture mechanics analysis predicated on the assumption of a wedge-loaded crack. Straightforward relationships among the alloys’ hardness (H), Palmqvist toughness (W), and fracture toughness ( $K_{IC}$ ) were also predicted by this research.

$$\text{Hardness (GPa)} = \frac{(1.8544 * \text{load})}{\text{diagonal average}^2} \quad (1)$$

where the load of indentation (N) and the diagonal average are measured in mm.

$$\text{Fracture Hardness}(K_{IC}) = 0.025 \left( \frac{E}{H} \right)^{0.4} (H \cdot W)^{0.5} \quad (2)$$

where  $K_{IC}$  is the indentation fracture toughness ( $\text{MPa} \cdot \text{m}^{1/2}$ ).  $W = \frac{P}{4a}$ , where P is the load of indentation (N), 2a is the Vickers diagonal (D), E = elastic modulus (GPa), and H = hardness (GPa).

### 3. Results and Discussion

The X-ray diffraction (XRD) technique of milled powder is used to analyze the peak broadening occurrence, crystal structure, and phase composition of materials after they have undergone mechanical milling or grinding processes and phase evolution after sintering. Non-agglomerated, ultra-fine (nano) Ti(CN) powder ranging from 200 nm to 350 nm in particle size was prepared via ball milling and subjected to XRD to study the peak broadening status of the as-received powder and the powder milled for various time intervals. The XRD results of the milled powder at different time periods are shown in Figure 1. The XRD peaks reveal the presence of Ti, C, and N phases. No foreign elements or

phase was identified in the ball-milled powders of different intervals. Peak broadening in XRD patterns is commonly observed as a result of size reduction, such as during mechanical milling. Peak broadening was observed after 5 h of the ball milling of Ti(CN) powder, and it increased to 30 h of ball milling. Peak broadening indicates size reduction. Peak broadening analysis of the XRD of the milled powder after 30 h shows a transition from micro to nano sizes, resulting in particle size reduction, which enhanced the densification during sintering, reduced the sintering time for a finer microstructure, and allowed more efficient atomic diffusion during the sintering, achieving high levels of densification and material properties. Scanning electron microscopy (SEM) energy dispersive X-ray spectroscopy (EDS) and transmission electron microscopy (TEM) analysis was performed on the powder milled for 30 h, as shown in Figure 2a–d. SEM with EDS is shown in Figure 2a,b, revealing a nano particle size and confirming the presence of the basic elements of Ti, C, and N. The TEM analysis image in Figure 2c,d shows a regular periodic arrangement of planes with crystalline phase and that the nanoparticles were dispersed uniformly. EDS in TEM confirmed the presence and distribution of titanium, carbon, and nitrogen within the nanoparticles. Thereafter, powders of the present composition were mixed in a WC jar at 500 rpm for 4 h.

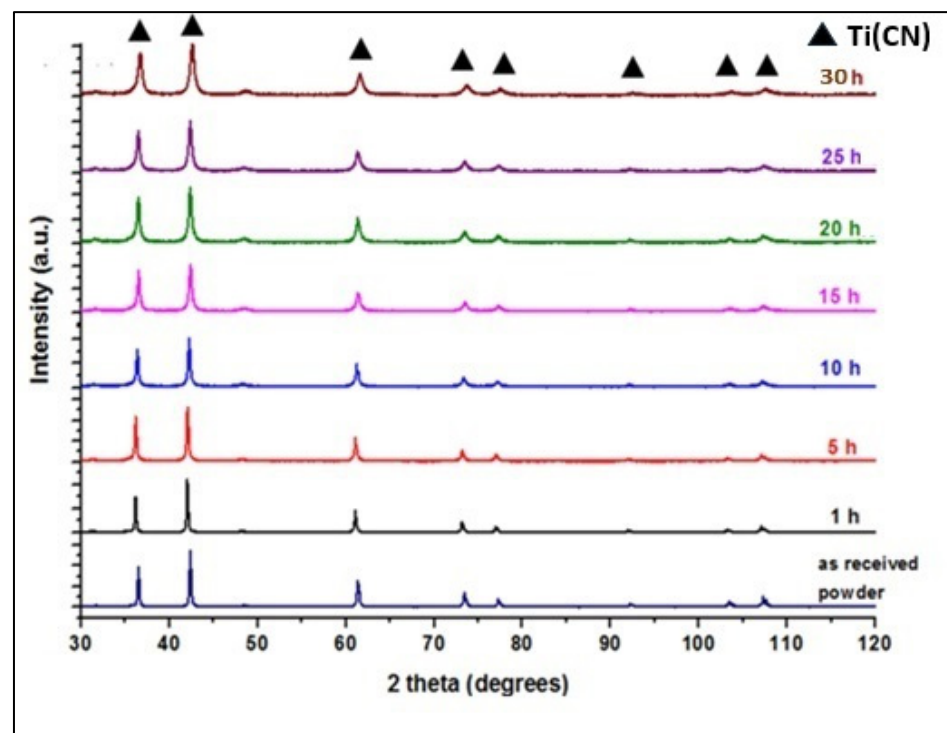


**Figure 1.** XRD analysis showing peaks of as-received and ball-milled Ti(CN) powder.

The densities of the sintered samples were measured by the Archimedes principle. The highest density of >98.5% was achieved for SPS-processed cermet at 1250 °C (Table 4). Via SPS, high levels of densification were achieved in the sintered material due to the combination of high temperature and pressure. SPS utilizes a pulsed DC to rapidly heat the powder compact, achieving temperatures close to or even above the melting point of the material within a short time. This rapid heating and cooling rate helps to minimize grain growth and retain finer microstructures. The dense microstructure contributes to improving the mechanical properties, including hardness. Liquid phase comprising Ni and Co effectively dissolves Ti(CN) and WC ceramic powders and precipitates out of ceramic solid solutions. Thus, the dissolution and reprecipitation process contributes to the densification [5,6]. The phase evolution in sintered 75TiCN-10WC-15(Ni-Co) cermet is represented in Figure 3a–c. Figure 3a,b shows the XRD of the SPS-processed cermet at

1250 °C and 1200 °C. Figure 3c shows the XRD pattern of the conventionally processed cermet at 1400 °C. XRD analyses for the investigated cermet revealed the presence of constituent elements and a solid solution, with some broadening in the SPS-processed cermet confirming a refined carbide size, as observed in the micrograph after sintering.

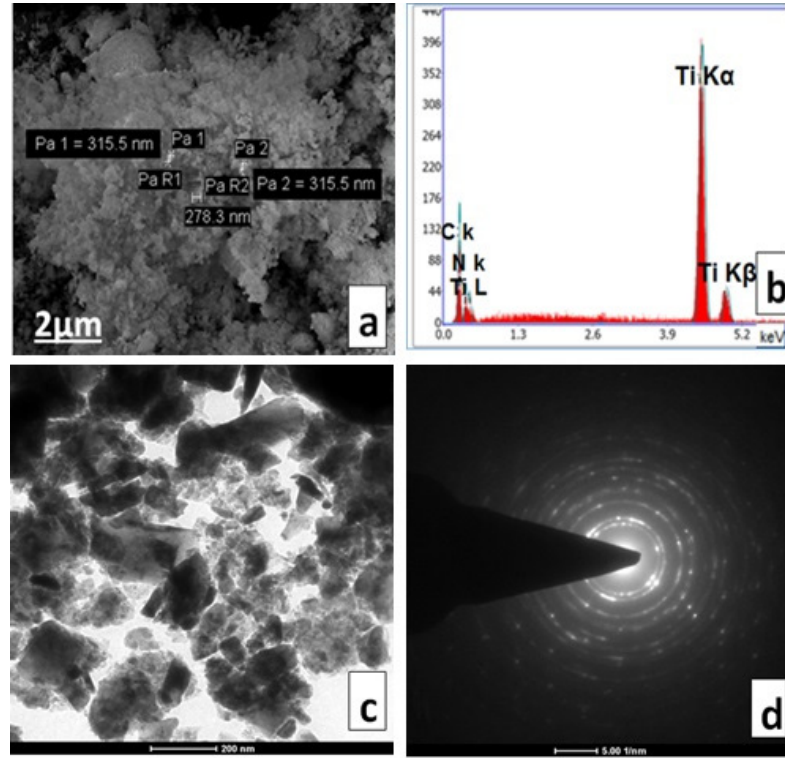


Figure 2. SEM (a); EDS (b), with TEM images of 30 h ball-milled Ti(CN) powder (c,d).

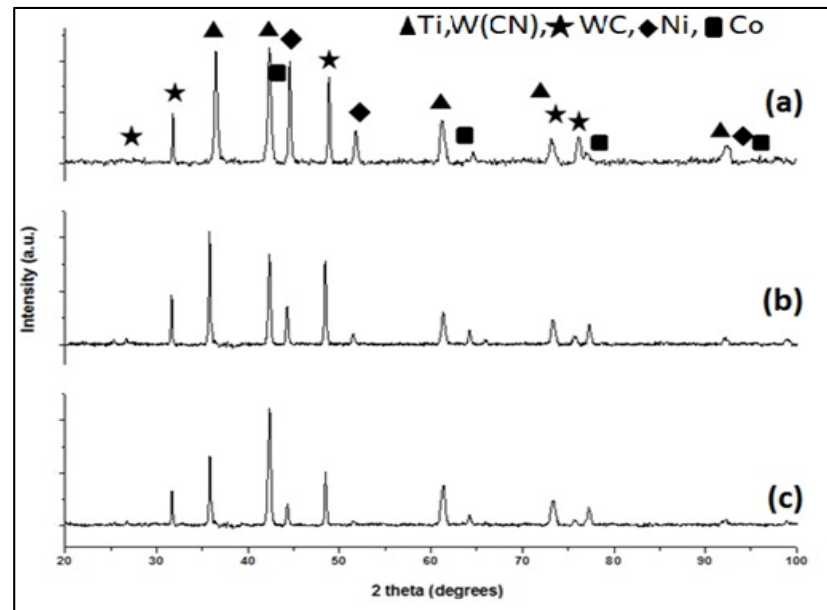
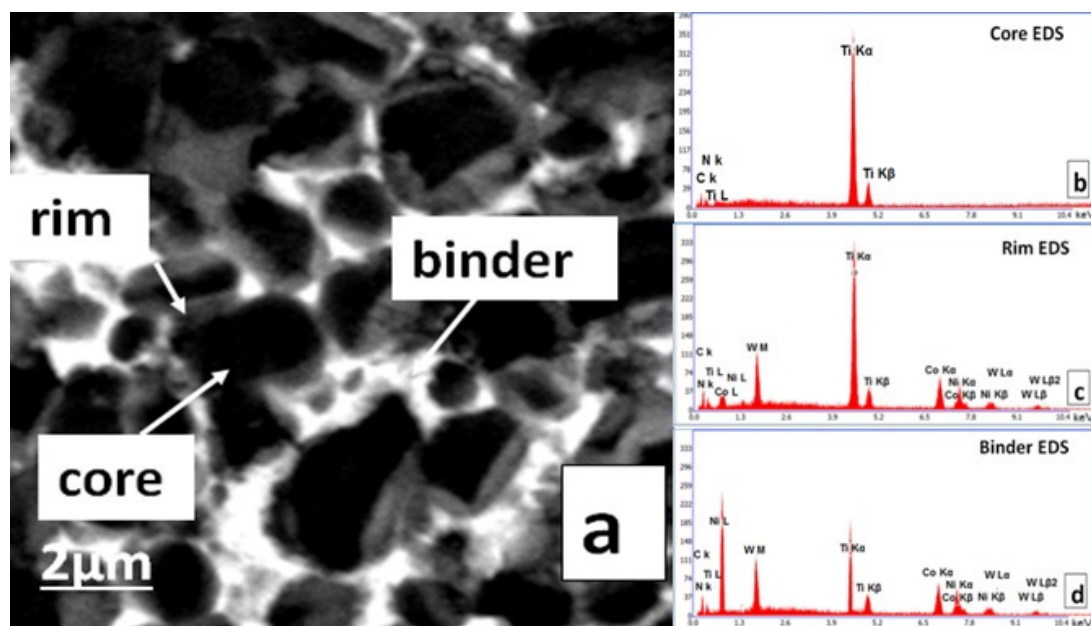


Figure 3. XRD patterns of sintered TiCN-based cermets: (a) SPS-processed at 1250 °C; (b) SPS-processed at 1200 °C; (c) conventionally sintered at 1400 °C.

**Table 4.** Properties of sintered nano Ti(CN)-based cermet.

Cermet (wt%): 75TiCN-10WC-15(Ni-Co)						
Sintering Technique	Sintering Temp. (°C)	Holding Time (min)	Pressure (MPa)	Relative Density (%)	HV10 (GPa)	K <sub>Ic</sub> (MPa m <sup>1/2</sup> )
Conventional	1400	60	150-uniaxial 300-isostatic	~98	15.0 ± 0.15	7.7 ± 0.45
SPS	1200	3	60	>98	15.8 ± 0.23	8.0 ± 0.30
	1250	3	60	>98.5	16.3 ± 0.34	8.5 ± 0.21

Figure 4a presents a micrograph of the conventionally sintered cermet at 1400 °C. The micrograph reveals that the core–rim morphology evolved due to the dissolution and reprecipitation process. Generally, there are three phases in cermets: the first is a hard phase, which is the core; the second is the surrounding phase—the rim; and the third one is a metal binder phase. EDS confirmed a typical core and rim structure, as shown in Figure 4b–d. Figure 4b reveals the presence of the Ti, C, and N elements in the core; in addition, W is also present in the rim (Figure 4c). Figure 4d reveals the major presence of the Ni and Co elements in the binder. Figure 5a,b shows a micrograph of the investigated cermet processed via spark plasma sintering at 1200 °C and 1250 °C. Figure 6a–d presents a micrograph of the results of the EDS of the SPS-processed cermet with the core, rim, and binder regions with their respective chemical compositions. It can be observed that SPS processing helped in achieving a high density with a reduced sintering time. Good bonding with clean boundaries are the benefits of SPS. With the simultaneous presence of pressure and an electric current, the sintering occurred very quickly, and consequently, the temperature increased, and densification was complete within few minutes. The novelty of multistage SPS is the activation of the grain boundaries; their diffusion, followed by lattice diffusion, results in good grain-to-grain bonding. SPS allows for the precise control over the sintering parameters, enabling the fabrication of materials with a controlled grain size and distribution. Fine-grained microstructures exhibit improved mechanical properties due to their increased grain boundary strengthening effect.

**Figure 4.** SEM (BSE) (a) and EDS (b–d) of core–rim–binder phases of conventionally processed Ti(CN)-based cermet at 1400 °C for 3 min.

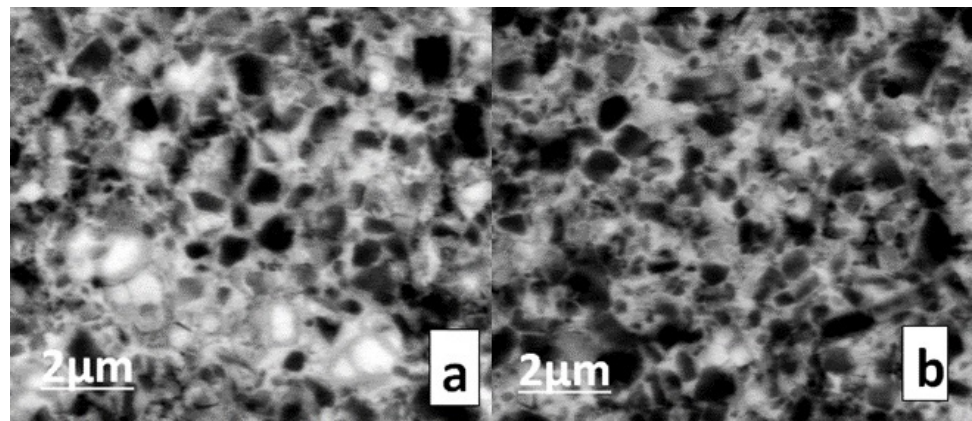


Figure 5. Micrograph of SPS cermet processed at 1200 °C (a) and 1250 °C (b).

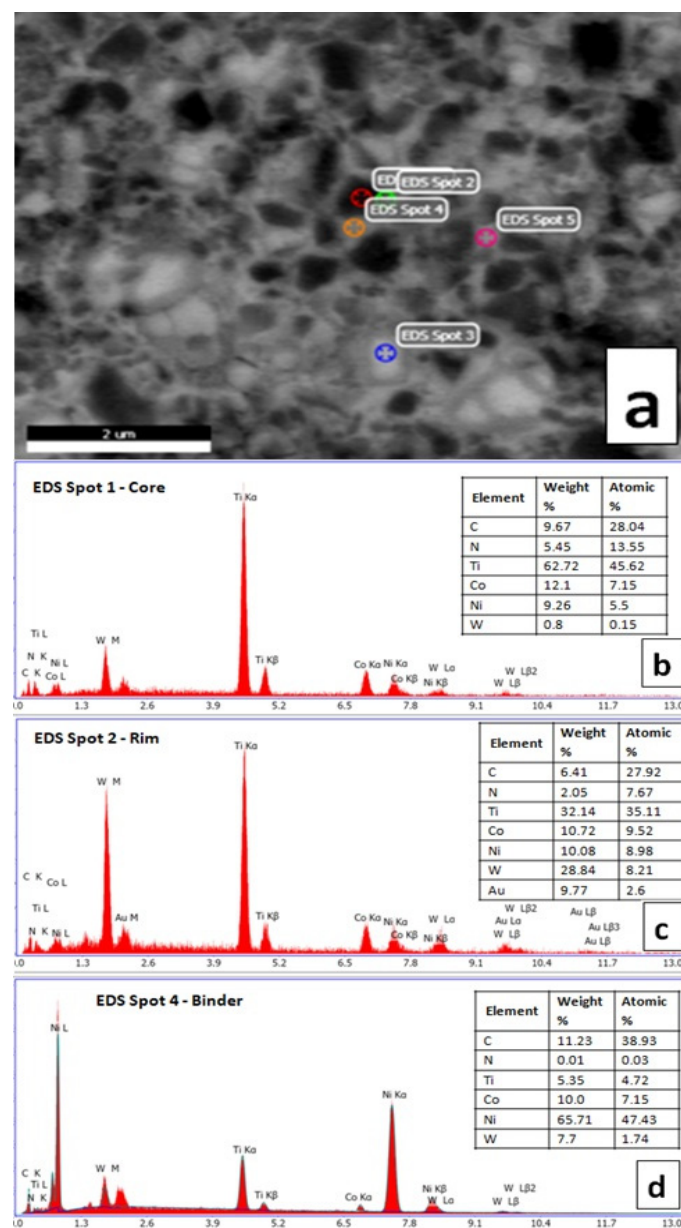


Figure 6. Micrograph of EDS of SPS-processed cermet (a) with the core (b), rim (c), and binder (d) regions with their respective chemical compositions.

It was found that the Vickers hardness for the Ti(CN)-based cermet processed via SPS at 1250 °C was ~16 GPa, and at 1200 °C, it was >15 GPa. The cermet processed via conventional sintering at 1400 °C was ~15 GPa (Table 1). The highest fracture toughness value of 8.5 MPa m<sup>1/2</sup> was achieved for the cermet processed via SPS at 1250 °C (Table 4). SPS is a fast densification route that prevents excessive grain growth, shortens the sintering temperature and time, and improves the properties of processed cermet. The short duration of the SPS process minimizes the diffusion of atoms along the grain boundaries, reducing the likelihood of segregation and the formation of secondary phases. This results in a more homogeneous microstructure with enhanced mechanical properties, including hardness.

#### 4. Conclusions

The present work focuses on the effects of conventional and spark plasma sintering on the physical and mechanical properties of advanced cermet systems. Nano Ti(CN)-based cermets with a 75TiCN-10WC-15(Ni-Co) composition were sintered via conventional sintering at 1400 °C for 60 min, where powder cermets were compacted in two stages (uniaxially at 100 MPa and further, isostatically, at 300 MPa), Multistage SPS was carried out at 1250 °C and 1200 °C for 3 min at 60 MPa in flowing argon. Nano Ti(CN) ranging from 200 nm to 315 nm in particle size was prepared by 30 h of ball milling. Peak broadening was observed after 5 h of ball milling, and it increased to 30 h of ball milling. The TEM results show a regular periodic arrangement of planes with crystalline phase. The highest density of >98.5% was achieved for the SPS-processed cermets. The XRD peaks of the SPS-processed cermet at 1250 °C show peak broadening, which confirms a refined carbide size. SEM micrographs revealed that the core–rim morphology evolved due to the dissolution and reprecipitation process. Hardness and fracture toughness was found to be high in the SPS-processed cermets. It is concluded that spark plasma sintering, in comparison to conventional sintering, offers significant advantages for the fabrication of nano Ti(CN)-based cermets, including high densification, fine microstructure control, enhanced mechanical properties, limited grain growth, and improved homogeneity.

**Author Contributions:** Conceptualization, M.G.-H. and V.V.; methodology, J.H.L.-D.; validation, J.H.L.-D., S.M.J. and R.C.C.; formal analysis, V.V.; investigation, V.V., M.G.-H., J.H.L.-D. and R.C.C.; resources, J.H.L.-D.; data curation, R.C.C.; writing—original draft preparation, V.V., J.H.L.-D. and E.J.S.-D.; writing—review and editing, J.H.L.-D. All authors have read and agreed to the published version of the manuscript.

**Funding:** This research did not receive external funding.

**Data Availability Statement:** The raw data supporting the conclusions of this article will be made available by the Authors on request.

**Conflicts of Interest:** The authors declare no conflict of interest. In particular, Vikas Verma, who is employed by the company Aqila Technologies and Integration Solutions Private Limited—Department of Aerospace Design & Operations, declares that the research was conducted in the absence of any commercial or financial relationships that could be construed as a potential conflict of interest.

#### References

1. Peng, Y.; Miao, H.; Peng, Z. Development of Ti(CN)-based cermets: Mechanical properties and wear mechanism. *Int. J. Refract. Met. Hard Mater.* **2013**, *39*, 78–89. [[CrossRef](#)]
2. Joardar, J.; Kim, S.W. Tribological Evaluation of Ultrafine Ti(CN) cermets. *Mater. Manuf. Process.* **2002**, *17*, 567–576. [[CrossRef](#)]
3. Soboyejo, W. Special Issue—Materials and Manufacturing Processes on Multifunctional Micro- and Nano-Structures. *Mater. Manuf. Process.* **2007**, *22*, 139. [[CrossRef](#)]
4. Kwona, W.T.; Park, J.S.; Kim, S.W.; Kang, S. Effect of WC and group IV carbides on the cutting performance of Ti(C,N) cermet tools. *Int. J. Mach. Tools Manuf.* **2004**, *44*, 341–346. [[CrossRef](#)]
5. Ettmayer, P.; Kolaska, H.; Lengauer, W.; Dreyer, K. Ti(C,N) Cermets—Metallurgy and Properties. *Int. J. Refract. Met. Hard Mater.* **1995**, *13*, 343–351. [[CrossRef](#)]
6. Shamanian, M.; Salehi, M.; Saatchi, A.; North, T.H. Influence of Ni Interlayers on the Mechanical Properties of Ti6Al4V/(WC-Co) Friction Welds. *Mater. Manuf. Process.* **2006**, *18*, 581–598. [[CrossRef](#)]

7. Ahn, S.Y.; Kang, S. Formation of core/rim structures in Ti(C,N)-WC-Ni cermets via a dissolution and precipitation process. *J. Am. Ceram. Soc.* **2003**, *83*, 1489–1494. [[CrossRef](#)]
8. Ahn, S.Y.; Kang, S. Effect of various carbides on the dissolution behavior of Ti(C<sub>0.7</sub>N<sub>0.3</sub>) in a Ti(C<sub>0.7</sub>N<sub>0.3</sub>)-30 Ni system. *Int. J. Refract. Met. Hard Mater.* **2001**, *19*, 539–545. [[CrossRef](#)]
9. Zhang, S. Titanium carbonitride-based cermets: Processes and properties. *Mater. Sci. Eng. A* **1993**, *163*, 141–148. [[CrossRef](#)]
10. Zhang, S.; Lu, G.Q. Sintering of Ti(C,N)Based Cermets: The Role of Compaction. *Mater. Manuf. Process.* **1995**, *10*, 773–783. [[CrossRef](#)]
11. Yoo, S.H.; Sethuram, K.M.; Sudarshan, T.S. Apparatus for Bonding a Particle Materials to Near Theoretical Density. U.S. Patent 5,989,487, 23 November 1999.
12. Yoo, S.H.; Sethuram, K.M.; Sudarshan, T.S. Method of Bonding a Particle Materials to Near Theoretical Density. U.S. Patent 6,001,304, 14 December 1999.
13. Alvarez, M.; Sánchez, J.M. Spark plasma sintering of Ti(C,N) cermets with intermetallic binder phases. *Int. J. Refract. Met. Hard Mater.* **2007**, *25*, 107–118. [[CrossRef](#)]
14. Ping, F.; Wei-hao, X.; Yong, Z.; Li-Xin, Y.; Yang-hua, X. Spark Plasma Sintering Properties of Ultrafine Ti (C, N)-based Cermet. *J. Wuhan Univ. Technol. Mater. Sci. Ed.* **2004**, *19*, 69–72. [[CrossRef](#)]
15. Zheng, Y.; Wang, S.; You, M.; Tana, H.; Xiong, W. Fabrication of nanocomposite Ti(C,N)-based cermet by spark plasma sintering. *Mater. Chem. Phys.* **2005**, *92*, 64–70. [[CrossRef](#)]
16. Srivatsan, T.S.; Manigandan, K.; Petraroli, M.; Trejo, R.M.; Sudarshan, T.S. Influence of size of nanoparticles and plasma pressure compaction on microstructural development and hardness of bulk tungsten samples. *Adv. Powder Technol.* **2013**, *24*, 190–199. [[CrossRef](#)]
17. Yoo, S.; Kalyanaraman, R.; Subhash, G.; Sudarshan, T.S.; Dowding, R.J. High Strain Rate Response of PAS (Plasma Activated Sintering) Consolidated Tungsten Powders, Materials Modification, Inc. Available online: [https://www.matmod.com/Publications/p2c\\_1.pdf](https://www.matmod.com/Publications/p2c_1.pdf) (accessed on 1 October 2002).
18. Shetty, D.K.; Wright, I.G.; Mincer, P.N.; Clauer, A.H. Indentation fracture of WC-Co cermets. *J. Mater. Sci.* **1985**, *20*, 1873–1882. [[CrossRef](#)]
19. Park, S.; Kang, S. Toughened ultra-fine (Ti,W)(CN)-Ni cermets. *Scr. Mater.* **2005**, *52*, 129–133. [[CrossRef](#)]
20. Jun, W.; Ying, L.; Yan, F.; Jinwen, Y.; Mingjing, T. Effect of NbC on the microstructure and sinterability of Ti(C<sub>0.7</sub>, N<sub>0.3</sub>)-based cermets. *Int. J. Refract. Met. Hard Mater.* **2009**, *27*, 549–551.
21. Zhang, X.; Liu, N.; Rong, C. Effect of molybdenum content on the microstructure and mechanical properties of ultra-fine Ti(C, N) based cermets. *Mater. Character.* **2008**, *59*, 1690–1696. [[CrossRef](#)]
22. Zhang, H.; Dikeb, Y.; Tang, S. Preparation and properties of ultra-fine TiCN matrix cermets by vacuum microwave sintering. *Rare Met.* **2010**, *29*, 528–532. [[CrossRef](#)]
23. Kim, Y.-S.; Kwon, W.T.; Seo, M.; Kang, S. Tool Performance of New Wear-resistant Cermets. *Int. J. Precis. Eng. Manuf.* **2012**, *13*, 941–946. [[CrossRef](#)]
24. Jeon, E.T.; Joardar, J.; Kang, S. Microstructure and tribo-mechanical properties of ultrafine Ti(CN) cermets. *Int. J. Refract. Met. Hard Mater.* **2002**, *20*, 207–211. [[CrossRef](#)]
25. Xiong, J.; Guo, Z.; Yang, M.; Shen, B. Preparation of ultra-fine TiC<sub>0.7</sub>N<sub>0.3</sub>-based cermet. *Int. J. Refract. Met. Hard Mater.* **2008**, *26*, 212–219. [[CrossRef](#)]
26. Liu, Y.; Jin, Y.; Yu, H.; Ye, J. Ultrafine (Ti, M)(C, N)-based cermets with optimal mechanical properties. *Int. J. Refract. Met. Hard Mater.* **2011**, *29*, 104–107. [[CrossRef](#)]
27. Jung, J.; Kang, S. Effect of ultra-fine powders on the microstructure of Ti(CN)-xWC-Ni cermets. *Acta Mater.* **2004**, *52*, 1379–1386. [[CrossRef](#)]
28. Xiong, J.; Guo, Z.; Shen, B.; Cao, D. The effect of WC, Mo<sub>2</sub>C, TaC content on the microstructure and properties of ultra-fine TiC<sub>0.7</sub>N<sub>0.3</sub> cermet. *Mater. Des.* **2007**, *28*, 1689–1694. [[CrossRef](#)]
29. Zhu, G.; Liu, Y.; Ye, J. Influence of Ce-Co pre-alloyed powder addition on the microstructure and mechanical properties of Ti(C, N)-based cermets. *Int. J. Refract. Met. Hard Mater.* **2013**, *37*, 134–141. [[CrossRef](#)]
30. Borrell, A.; Salvador, M.D.; Rocha, V.G.; Fernández, A.; Aviles, M.A.; Gotor, F.J. Bulk TiC<sub>x</sub>N<sub>1-x</sub>-15%Co cermets obtained by direct spark plasma sintering of mechanochemical synthesized powders. *Mater. Res. Bull.* **2012**, *47*, 4487–4490. [[CrossRef](#)]
31. Gong, J.; Pan, X.; Miao, H.; Zhao, Z. Effect of metallic binder content on the microhardness of TiCN-based cermets. *Mater. Sci. Eng. A* **2003**, *359*, 391–395. [[CrossRef](#)]
32. Liu, N.; Yin, W.; Zhu, L. Effect of TiC/TiN powder size on microstructure and properties of Ti(C, N)-based cermets. *Mater. Sci. Eng. A* **2007**, *445–446*, 707–716. [[CrossRef](#)]
33. Zheng, Y.; Xiong, W.; Liu, W.; Lei, W.; Yuan, Q. Effect of nano addition on the microstructures and mechanical properties of Ti(C, N)-based cermets. *Ceram. Int.* **2005**, *31*, 165–170. [[CrossRef](#)]
34. Liu, N.; Han, C.; Xu, Y.; Chao, S.; Shi, M.; Feng, J. Microstructures and mechanical properties of nano TiN modified TiC-based cermets for the milling tools. *Mater. Sci. Eng. A* **2004**, *382*, 122–131. [[CrossRef](#)]
35. Xiong, J.; Guo, Z.; Wen, B.; Li, C.; Shen, B. Microstructure and properties of ultra-fine TiC<sub>0.7</sub>N<sub>0.3</sub> cermet. *Mater. Sci. Eng. A* **2006**, *416*, 51–58. [[CrossRef](#)]

36. Cardinal, S.; Malchère, A.; Garnier, V.; Fantozzi, G. Review Microstructure and mechanical properties of TiC–TiN based cermets for tools application. *Int. J. Refract. Met. Hard Mater.* **2009**, *27*, 521–527. [[CrossRef](#)]
37. Yun, H.; Zou, B.; Wang, J. Effects of sintering temperature and nano Ti(C,N) on the microstructure and mechanical properties of Ti(C,N) cermets cutting tool materials with low Ni-Co. *Mater. Sci. Eng. A Struct.* **2017**, *705*, 98–104. [[CrossRef](#)]
38. Zhang, G.; Huang, M.; Zhao, H.; Zhang, H.; Wang, Y.; Zhang, X.; Zheng, H.; Lu, P.; Zhao, Z. Investigation and properties of Ti(C,N)-based cermets with graphene nanosheet addition by spark plasma sintering. *J. Mater. Res. Technol.* **2023**, *24*, 185–199. [[CrossRef](#)]
39. Yan, H.; Deng, Y.; Su, Y.Y.; Jiang, S.; Chen, Q.W.; Cao, S.X.; Liu, B. Ti(C, N)-Based Cermets with Two Kinds of Core-Rim Structures Constructed by  $\beta$ -Co Microspheres. *Adv. Mater. Sci. Eng.* **2020**, *1–11*, 4684529. [[CrossRef](#)]
40. Shankar, E.; Prabu, S.B.; Padmanabhan, K.A. Mechanical properties and microstructures of TiCN/nano-TiB<sub>2</sub>/TiN cermets prepared by spark plasma sintering. *Ceram. Int.* **2018**, *44*, 9384–9394. [[CrossRef](#)]
41. Zhang, M.M.; Jiang, Y.; Lin, N.; Kang, X.Y.; Yan, Y.; Huang, J.H.; Liu, Y.; Qiu, S.; He, Y.H. Investigation of the oxidation behavior and high oxidation-resistant mechanism of Ti(C,N)-based cermets. *Corros. Sci.* **2020**, *177*, 108959. [[CrossRef](#)]
42. De la Odra, A.G.; Sayagués, M.J.; Chicardi, E.; Gotor, F.J. Development of Ti(C,N)-based cermets with (Co,Fe,Ni)-based high entropy alloys as binder phase. *J. Alloys Compd.* **2019**, *814*, 152218. [[CrossRef](#)]
43. Subin, A.J.; Merbin, J.; Menezes, P.L. Cermet Systems: Synthesis, Properties, and Applications. *Ceramics* **2022**, *5*, 210–236. [[CrossRef](#)]
44. Comstock, G.J. Hard Cemented Carbide Material. U.S. Patent 2,033,513, 10 March 1936.
45. Santrade, Ltd. Wear Resistant Alloy. U.S. Patent 4,145,213, 20 March 1979.
46. Kennametal, Inc. Cermet Cutting Tool. U.S. Patent 4,942,097, 17 July 1990.
47. Watanabe, T.; Doutsu, T.; Yagishita, O.; Yamamoto, H.; Kai, Y.; Agency of Industrial Science. Titanium Carbo-Nitride and Chromium Carbide-Based Ceramics Containing Metals. U.S. Patent 4,948,425, 14 August 1990.
48. Isobe, K.; Nomura, T. Cermet Alloy Containing Nitrogen. U.S. Patent 5,186,739, 16 February 1993.
49. Teruuchi, K.; Ueda, F.; Odani, N. Wear Resistant Titanium Carbonitride-Based Cermet Cutting Insert. U.S. Patent 5,370,719, 6 December 1994.
50. Weinl, G.; Oskarsson, R.; Hultman, L. Titanium-Based Carbonitride Alloy with Controlled Structure. U.S. Patent 5,395,421, 7 March 1995.
51. Nakamura, S.; Fujisawa, T.; Teruuti, K.; Tsujisaki, H.; Nonaka, M. Cutting Blade Made of Titanium Carbonitride-Base Cermet, and Cutting Blade Made of Coated Cermet. U.S. Patent 5,766,742, 16 June 1998.
52. Rolander, U.; Weinl, G.; Lindahl, P.; Andren, H.O. Titanium-Based Carbonitride Alloy with Controllable Wear Resistance and Toughness. U.S. Patent 6,004,371, 21 December 1999.
53. Iyori, Y.; Nakahara, Y.; Kimura, Y. TiCN-Based Cermet. U.S. Patent 6,387,552 B1, 14 May 2002.
54. Mitsubishi Materials Corp. Cermet Cutting Insert. European Patent Application EP 1,043,414 A1, 5 April 2000.
55. Weinl, G.; Rolander, U.; Zwinkels, M. Ti(C,N)-(Ti,Nb,W)(C,N)-Co Alloy for Milling Cutting Tool Applications. U.S. Patent 7,332,122 B2, 19 February 2008.
56. Lee, H.H.; Kim, K.H.; Shin, S.J.; Kim, S.M. Method for Producing Titanium Carbonitride Powder. European Patent EP3,181,274B1, 18 December 2019.
57. Rolander, U.; Zwinkels, M.; Weinl, G. Ti(C,N)-(Ti,Nb,W)(C,N)-Co Alloy for Finishing and Semi finishing Turning Cutting Tool Applications. U.S. Patent 7,645,316 B2, 12 January 2010.
58. Mitsubishi Materials Corp. Cermet Insert and Cutting Tool. U.S. Patent 8,007,561 B2, 30 August 2011.
59. Banerjee, D. Cemented Carbide with Ultra-Low Thermal Conductivity. U.S. Patent 8,202,344 B2, 19 June 2012.

**Disclaimer/Publisher’s Note:** The statements, opinions and data contained in all publications are solely those of the individual author(s) and contributor(s) and not of MDPI and/or the editor(s). MDPI and/or the editor(s) disclaim responsibility for any injury to people or property resulting from any ideas, methods, instructions or products referred to in the content.